

A Potential Roadmap to Integrated Metal Organic Framework Artificial Photosynthetic Arrays

Bradley Gibbons, Meng Cai, and Amanda J. Morris*



Cite This: *J. Am. Chem. Soc.* 2022, 144, 17723–17736



Read Online

ACCESS |

Metrics & More

Article Recommendations

ABSTRACT: Metal organic frameworks (MOFs), a class of coordination polymers, gained popularity in the late 1990s with the efforts of Omar Yaghi, Richard Robson, Susumu Kitagawa, and others. The intrinsic porosity of MOFs made them a clear platform for gas storage and separation. Indeed, these applications have dominated the vast literature in MOF synthesis, characterization, and applications. However, even in those early years, there were hints to more advanced applications in light–MOF interactions and catalysis. This perspective focuses on the combination of both light–MOF interactions *and* catalysis: MOF artificial photosynthetic assemblies. Light absorption, charge transport, H₂O oxidation, and CO₂ reduction have all been previously observed in MOFs; however, work toward a fully MOF-based approach to artificial photosynthesis remains out of reach. Discussed here are the current limitations with MOF-based approaches: diffusion through the framework, selectivity toward high value products, lack of integrated studies, and stability. These topics provide a roadmap for the future development of fully integrated MOF-based assemblies for artificial photosynthesis.

1. INTRODUCTION

One of the greatest challenges facing the scientific community today is the search for a sustainable, renewable energy source to match increasing global energy demands. As research into new forms of energy continues, nature can provide inspiration for utilizing one of the most abundant renewable sources—sunlight. Through photosynthesis, plants store solar energy in chemical bonds, using abundant starting materials like H₂O and CO₂. The stored energy can be accessed at any time, providing a constant supply of energy despite the temporal nature of sunlight. For this reason, photosynthesis is one of the most promising avenues of utilizing solar energy on a large scale. While plants have had eons to perfect the process, attempts to artificially replicate photosynthesis still face great challenges. Significant work has been done to address some of these challenges, making artificial photosynthesis a large area of research today.^{1,2}

Photosynthesis requires a number of complex interactions including the following: light absorption (at two spatially separated photosystems); oxidation of water to oxygen and protons; a complex electron transport chain through and across the thylakoid membrane; and finally, transport of NADPH outside the thylakoid membrane for the reduction of carbon dioxide into carbohydrates for long-term energy storage. Individually, light absorption, directed energy and charge transport, and multielectron redox reactions can be accomplished in the lab, but it remains challenging to combine these functions into one assembly. Two prevailing examples of integrated artificial photosynthetic assemblies are dye-sensitized photoelectrochemical cells (DSPECs) pioneered by Thomas Meyer and multijunction solid state approaches like those of JCAP (Joint Center for Artificial Photosynthesis) and NREL (National Renewable Energy Lab) (Figure 1).^{3,4}

DSPECs are envisioned to utilize metal oxides (such as n-TiO₂ and p-NiO) coupled with molecular catalysts to drive water oxidation and proton reduction.⁴ These hybrid systems have progressed rapidly since their conception in 1999 and now contain multiple molecular components to enhance both catalysis and light absorption. On the other hand, approaches by JCAP and NREL focus on multifunctional photoelectrodes, such as a recent device utilizing a Rh-catalyst-modified TiO₂ cathode and RuO_x anode for direct water splitting with a 19% solar-to-hydrogen efficiency.⁵ While both approaches have been successful in harvesting solar energy and driving catalytic reactions, knowledge gaps remain that prevent translation to technology. Top limitations that exist in the field include: (1) diffusion to and from catalytically active surfaces; (2) stability to light, pH, and other working conditions; (3) selectivity and efficiency toward complex, high-value products; and (4) the need for integrated studies. As the field advances toward the goal of large-scale solar energy production, these challenges must be addressed for every approach.

A new platform for artificial photosynthesis has recently emerged: metal organic frameworks (MOFs). MOFs are a class of crystalline materials composed of inorganic ions or clusters bridged by organic linkers to form highly porous structures in one, two, or three dimensions. MOFs incorporate high levels of tunability with stability in a variety of environments. Because

Published: September 20, 2022



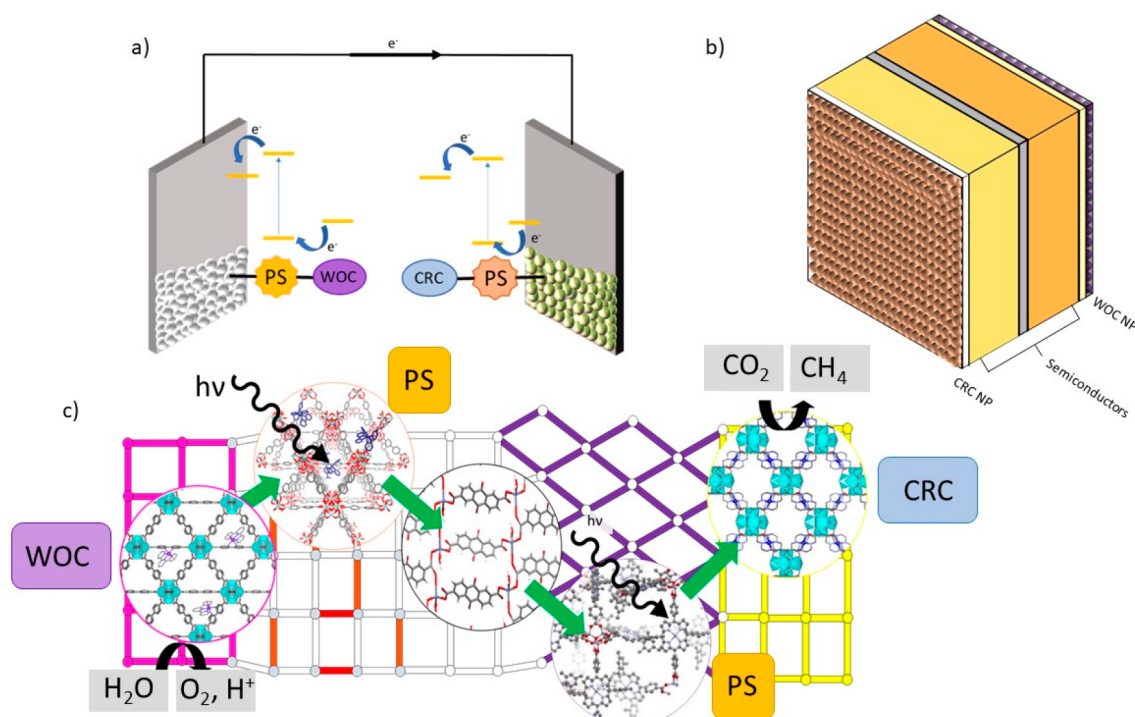


Figure 1. Schematics for artificial photosynthetic assemblies showing DSPECs featuring a photosensitizer (PS), water oxidation catalyst (WOC), and CO_2 reduction catalyst (CRC) (a), multijunction semiconductors with catalytic nanoparticles (NP) (b), and a proposed all-MOF artificial photosynthetic assembly (c). Figure created using VESTA visualization software.¹³⁴

MOFs are still relatively new, the MOF community has the unique opportunity to explore MOF artificial photosynthetic chemistry through the lens of the challenges not yet addressed by previous artificial photosynthetic approaches. MOF structures with all of the necessary functions for artificial photosynthesis, including light harvesting, energy transfer, electron and proton transport, and catalysis (Figure 1), can be envisioned.⁶ We firmly believe MOFs can build on knowledge gained by existing systems to create highly stable, molecular, integrated artificial photosynthetic assemblies. Notwithstanding, the fundamental knowledge gained through MOF assemblies will continue to drive the broader field of artificial photosynthesis forward.

Significant work has been done with MOFs driving one aspect of artificial photosynthesis (e.g., water oxidation,^{7–14} carbon dioxide reduction,^{15–19} proton reduction^{20–22}). In addition to driving catalytic reactions, MOFs have been investigated for light harvesting^{23–30} and charge transport.^{31–35} Initial work demonstrated enhanced catalyst stability and long-range energy transfer, which established MOFs as a viable platform for artificial photosynthetic chemistry.⁶ Here, we discuss the present fundamental challenges in the field of MOF-based artificial photosynthesis. Topics include substrate and product diffusion through frameworks, selectivity toward high value products, the lack of integrated studies, and the stability of MOFs under reaction conditions. While some approaches to artificial photosynthesis focus on proton reduction to hydrogen, the discussion presented here will largely be limited to the conversion of carbon dioxide to other carbon-based products. Additionally, there may be other technical concerns regarding device fabrication or electronic connections at interfaces, but they are beyond the scope of this perspective.

2. THE STATE OF THE FIELD

Artificial photosynthesis, as defined herein, couples the oxidation of water to the reduction of carbon dioxide. Additionally, there is a spatial consideration to the chemistry—specifically, for relevant chemistry the reduction of CO_2 should be spatially separated from the oxidation of H_2O . If the two half reactions occur at one particle, the oxygen produced will likely quench any CO_2 reduction activity. With these constraints in mind, there are no examples of artificial photosynthetic chemistry by a spatially separated MOF assembly. That said, there is an elegant example of photocatalytic total water splitting, where the CO_2 reduction reaction is replaced with the reduction of protons to hydrogen.³⁶ We also note that there are examples of purely electrochemical total water splitting by MOFs.^{37,38} While not identical, many aspects of artificial photosynthesis can be found in water splitting, and the recent demonstrations will help set the groundwork for a full MOF artificial photosynthetic array.

For photocatalytic water splitting at spatial separated MOF-components, Hu et al. integrated light-harvesting and catalysts-containing MOF-nanosheets on either the interior or exterior of a liposome vesicle (Figure 2).³⁶ Water oxidation was carried out in the hydrophilic interior of the vesicle by a Zr-based framework with two bipyridine-linked functional components: a ruthenium photosensitizer and an iridium-based catalyst. Proton reduction occurred in the hydrophobic vesicle bilayer using a Hf-based porphyrinic framework containing a mixture of Zn and Pt porphyrins as photosensitizer and catalyst, respectively. Two redox couples were used as an electron transport chain, delivering electrons generated during water oxidation to the catalytic porphyrin centers for hydrogen reduction. The overall quantum yield was limited to 1.5%, due to the slow rate of proton reduction (compared to water

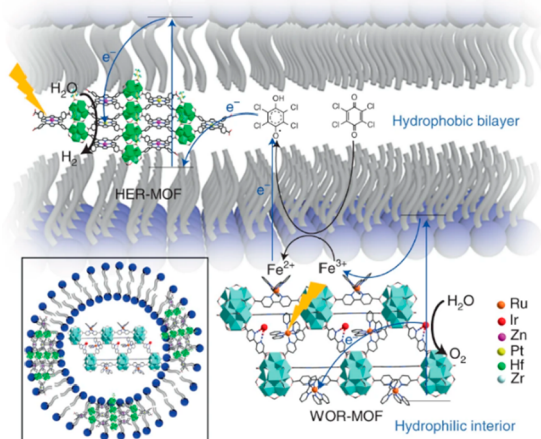


Figure 2. Illustration of photocatalytic water splitting by MOF-based catalysts immobilized in a liposome vesicle with a hydrogen evolution catalyst imbedded into the hydrophobic bilayer and the water oxidation catalyst located in the hydrophilic interior. Reprinted with permission from ref 36. Copyright 2021 Springer Nature.

oxidation) and charge transport across the membrane. This example elicits further questions for the MOF field. Namely, is it possible to create a complete MOF approach that incorporates charge transport through a proton-conducting MOF membrane, as opposed to the use of small molecule mediators? Can limitations in charge and mass transport in MOFs be eliminated? Can true artificial photosynthesis be achieved through the coupling of H₂O oxidation to CO₂ reduction?

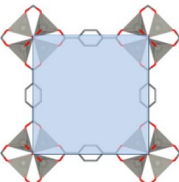
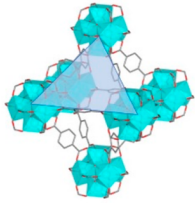
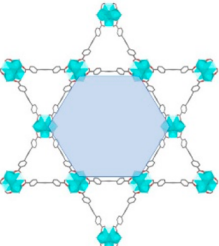
3. TRANSPORT PHENOMENA

The large internal surface area of MOFs is usually considered a benefit over other heterogeneous catalytic systems. While typical metal oxide based catalysts have surface areas of 100–300 m²/g, MOFs have been reported to have surface areas as high as 7800 m²/g, providing access and inclusion of significantly more reaction sites.^{39,40} However, this potential can only be realized if catalysis occurs throughout the framework and not just on the exterior surface. As a result, the diffusion of substrates and products through MOF pores is a critical parameter to consider. Catalysis may occur in a relatively dilute substrate environment (typically seen with carbon dioxide reduction), or a highly concentrated one (water oxidation), but in both cases the goal is to be limited by catalytic turnover rather than diffusion processes.

3.1. Diffusion of Neutral Species. The reactions occurring in artificial photosynthesis largely involve small molecules as both substrates (CO₂, H₂O) and products (O₂, H₂, CO, HCOOH, CH₃OH, etc.). However, even for small molecules, their reported mass transport diffusion coefficients in MOFs are small compared to solution based values (10⁻⁹–10⁻¹⁴ cm²/s in MOFs compared to 10⁻⁵ cm²/s in solution).^{41,42} Mass transport in MOFs still appears to largely follow Fickian diffusion models, and is directly related to the relative size of the diffusing substrate and the MOF channel or pore window. For molecules that are relatively small, diffusion will occur throughout the framework and total penetration of the substrate can occur. However, for large substrates, diffusion throughout the framework is slow, and some large species cannot penetrate into the interior of the framework.¹⁴ A good approximation of reagent size restriction can be made from

basic geometric calculations that show that the maximum radius of a sphere that can enter a MOF pore of specific geometry (Table 1). This basic geometric calculation can be

Table 1. Geometric Calculations for the Radius of an Inscribed Circle for Various Geometric Shapes Common in MOFs

Pore Geometry	Equation	Example
Rectangle	$r = \frac{h}{2}$ h=height	MOF-5 
Triangle	$r = \frac{a\sqrt{3}}{6}$ a=edge length	UiO-66 
Hexagon	$r = \frac{a\sqrt{3}}{2}$ a=edge length	NU-1000 

useful when considering reagent choice for different MOFs. For example, ceric ammonium nitrate (CAN) is a common sacrificial oxidant used in water oxidation reactions; however, its large size (~5.65 Å radius) might limit diffusion into smaller MOFs. Even considering the size of the relevant aqueous species [Ce(OH₂)₆]²⁺ (~2.8 Å radius), diffusion into confined, solvated MOF pores may be difficult. Indeed, when used with UiO-67 (r_{max} = 2.90 Å), it appears that diffusion into the MOF interior is virtually nonexistent and all catalytic activity is due to surface bound catalysts.¹⁴ When the MOF linker is expanded to accommodate larger substrates (r_{max} = 5.34 Å), limited CAN diffusion can occur into the MOF interior.¹³ For these calculations it is important to remember that geometric constraints represent a *theoretical maximum* size for substrates to enter. Diffusion into solvated MOFs is more difficult, and as a result the actual maximum substrate size that can enter a given pore is smaller.

One might assume then that the design of MOFs with larger pore windows would be sufficient to overcome diffusion barriers. However, even in larger UiO-type frameworks,

diffusion of the CAN is on the order of 10^{-11} cm²/s, several orders of magnitude lower than in solution.¹³ Studies on diffusion through MOFs suggest that if the pore size is at least 4 times the size of the substrate, further pore size increases will only marginally increase diffusion rates.⁴⁴ Put simply, even in large pore structures, substrates must diffuse through a confined environment, which will often substantially differ from diffusion through bulk solvent. Additionally, framework topology will also have significant effects on the overall diffusion rate, and maximum loading of substrates into the MOF.^{45,46} Large, open channels running along a single axis may promote faster diffusion and allow for larger substrates to enter, but is generally less efficient at overall substrate loading compared to 3D diffusion through smaller pores. This is illustrated by confocal microscopy measurements of a fluorescent dye into the pores of MOFs with different topology (Figure 3).⁴⁵ Although the calculated diffusion coefficient is

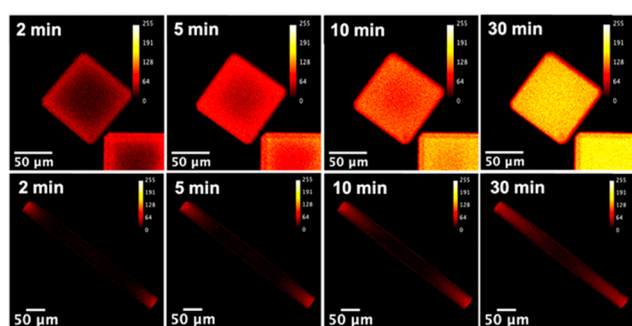


Figure 3. Time resolved confocal microscopy of dye diffusion into MOFs of different morphologies. While some frameworks may have larger channels to promote diffusion in one direction (bottom), overall loading can be limited since diffusion is limited to one direction. Reprinted with permission from ref 45. Copyright 2021 American Chemical Society.

higher for the rod-like NU-1008 (Figure 3, bottom), the cubic NU-600 (Figure 3, top) shows significantly more dye loading at the same time points. Although NU-1008 contains a much larger pore (diameter = 30), diffusion only occurs along a single axis, and there is no diffusion between pores. In NU-600 (diameter = 19 Å), there is an intersecting network of pores, which gives a lower diffusion coefficient, but higher loading of substrate at the same time point. It may be possible to achieve the best of both worlds by controlling the aspect ratio of rod-like crystallites, but this often presents a new synthetic challenge. Other factors, such as MOF-substrate interactions, external surface barriers, and solvent structure may also have dramatic effects on the rate of diffusion and framework capacity.^{41,47,48}

3.2. Ion and Proton Transport. Beyond concerns over mass transport in MOFs, artificial photosynthesis relies heavily on efficient charge transport (both electrons and protons) to drive efficient redox reactions. In natural photosynthesis, this is largely accomplished by a series of redox active quinones, which accept electrons from excited chlorophyll and shuttle protons generated in water oxidation to photosystem I for the reduction of NADP⁺. The directed transport of protons and electrons from light harvesting chlorophyll to NADPH is critical for the reduction of carbon dioxide, which occurs in the chloroplast. Similarly, in a MOF-based artificial photosynthetic assembly, the light harvesting components are often spatially separated from catalytic centers. Directed transport of protons

and electrons is critical for activation of interior catalytic sites and highly selective and efficient catalysis.⁴⁹

One approach to promoting proton transport in MOFs is through the synthesis of charged frameworks, composed of ionic nodes accompanied by charge balancing ions that saturate the pores.⁵⁰ As a result, extensive H-bond networks between the incorporated counterions, MOF nodes, and protic solvent form an efficient pathway for the proton-hopping (or Grotthuss) mechanism of diffusion. Fe-CAT-5 for example displays proton conductivity (5×10^{-2} S/cm) nearly as high as the commercial standard of Nafion (10^{-1} S/cm).⁵¹ Composed of Fe(C₂O₂)₃ nodes and H₆THO (THO₆⁻ = triphenylene-2,3,6,7,10,11-hexakis(olate)) linkers, Fe-CAT-5 is an interpenetrated framework, with each framework connected by a bridging Fe₂(SO₄)₂ cluster (Figure 4a). The nodes are charge

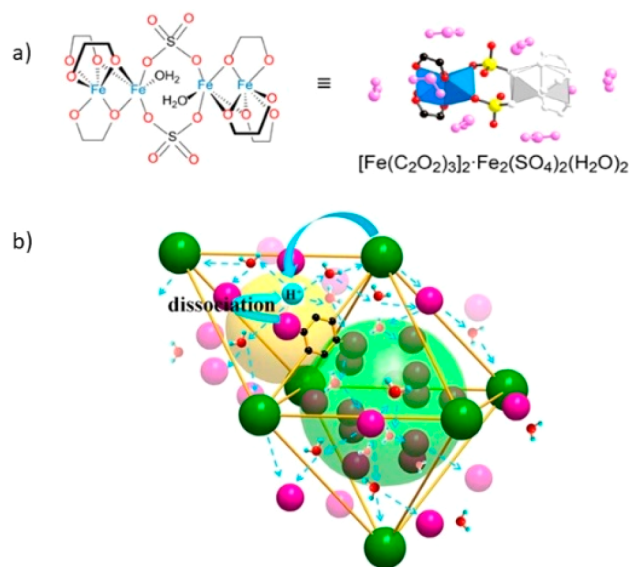


Figure 4. Examples of proton conductivity through a charged node in Fe-CAT-5 (a) and linker modification of an insulating framework like UiO-66 with $-\text{SO}_3\text{H}$ (pink spheres) groups (b). Reprinted with permission from refs 51 and 53. Copyright 2015 American Chemical Society.

balanced by dimethylamine (DMA) ions in the pores, and both DMA and sulfate ions contribute to the long-range H-bonding network and high proton conductivity. Other charged frameworks have demonstrated conductivity over a range of relative humidity and temperatures, due to an extensive hydrogen bond network between aqua ligands coordinated to the MOF node.⁵²

An alternative strategy to facilitate ionic diffusion is to modify MOF ligands and/or nodes to improve protonic and ionic conductivity over the parent framework.^{54–60} For example, charged frameworks isostructural with HKUST-1 have been synthesized by replacing the oxygen atoms in the paddle-wheel node with chloride ions. The Co analogue $[\text{Co}_2\text{Cl}_2(\text{BTC})_{4/3}](\text{Me}_2\text{NH}_2)_2$ demonstrates high proton conductivity (5.93×10^{-4} S/cm) compared to the neutral framework (1.5×10^{-5} S/cm).^{55,56} Other node modifications involve the addition of proton carrier molecules such as imidazole or sulfamate to MOF nodes, providing H-bonding sites for structured solvent in the MOF pores.^{58,59} Similarly, MOF linkers have been functionalized with $-\text{OH}$, $-\text{COOH}$, $-\text{NH}_2$, $-\text{SH}$, or $-\text{SO}_3\text{H}$ groups resulting in proton

conductivities on the order of 10^{-3} – 10^{-1} S/cm (Figure 4b).^{53,57} Since proton conductivity is directly related to the mobility of protons, functionalization with highly acidic functional groups (such as sulfonic acid), which are more fully dissociated, generally show increased conductivity over weaker acids. Finally, MOF conductivity can be increased through host–guest interactions by the incorporation of proton carrier molecules into the MOF pores, rather than bound to the ligand or node.^{61,62} These structures can achieve high levels of conductivity (10^{-1} S/cm), but come at the trade-off of lower porosity and available surface area, since the MOF pore is loaded with the proton carriers.⁶³

Similar to proton transport, movement of electrons and counterions are critical for driving the redox reactions of water oxidation. In redox reactions, these two processes are normally described by the apparent diffusion coefficient (D_{app}), but they can be separated to better understand the limits of electrochemical charge transport in MOFs. Transport of electrons between redox active centers isolated within a MOF is dictated by a redox hopping mechanism, where electrons hop from redox site to redox site across the framework.⁶⁴ This process is largely dictated by the distance between redox sites, and the self-exchange rate of the organometallic complex. However, studies on electron transport in MOFs suggest that the rate limiting step is not the electron hopping rate (10^{-9} – 10^{-10} cm²/s), but rather the diffusion of the accompanying counterion to maintain charge neutrality (10^{-11} – 10^{-14} cm²/s).^{44,65} Counter ion diffusion rates can be improved by choice of ion or, to an extent, increasing the pore size of the MOF. It should be noted that these measurements only consider transport of ions *into* the framework. At a steady state, counterions are present *within* the MOF pores, and it is likely that the limiting process will become the self-exchange rate of the redox center used for catalysis.

4. SELECTIVITY AND EFFICIENCY

Ideal artificial photosynthetic catalysts need to be both highly efficient for the desired reaction and selective toward a specific product. In some cases, such as water oxidation, selectivity is not generally an issue; however, this is not the case for carbon dioxide reduction. Hydrogen evolution (0.00 V vs NHE, pH = 0)⁶⁶ occurs readily under the conditions required for carbon dioxide reduction. In addition to a lower energetic requirement than some carbon dioxide reduction pathways (see Table 2), hydrogen evolution is typically favored due to the relatively low concentrations of dissolved carbon dioxide in acidic aqueous solutions. Even when carbon dioxide reduction occurs, the wide range of potential reduction pathways often results in the formation of multiple products. One classic example from outside the MOF field is the use of copper,

Table 2. Potentials for Select CO₂ Electrochemical Reduction Products (vs SHE, pH = 0)^{66,71}

$2\text{H}^+ + 2\text{e}^- \rightleftharpoons \text{H}_{2(\text{g})}$	0.00 V
$\text{CO}_2(\text{g}) + 2\text{H}^+ + 2\text{e}^- \rightleftharpoons \text{HCOOH}(\text{l})$	−0.25 V
$\text{CO}_2(\text{g}) + 2\text{H}^+ + 2\text{e}^- \rightleftharpoons \text{CO}(\text{g}) + \text{H}_2\text{O}(\text{l})$	−0.11 V
$\text{CO}_2(\text{g}) + 6\text{H}^+ + 6\text{e}^- \rightleftharpoons \text{CH}_3\text{OH}(\text{l}) + \text{H}_2\text{O}(\text{l})$	+0.02 V
$\text{CO}_2(\text{g}) + 8\text{H}^+ + 8\text{e}^- \rightleftharpoons \text{CH}_4(\text{g}) + 2\text{H}_2\text{O}(\text{l})$	+0.17 V
$2\text{CO}_2(\text{g}) + 2\text{H}^+ + 2\text{e}^- \rightleftharpoons \text{H}_2\text{C}_2\text{O}_4(\text{aq})$	−0.50 V
$2\text{CO}_2(\text{g}) + 12\text{H}^+ + 12\text{e}^- \rightleftharpoons \text{CH}_2\text{CH}_2(\text{g}) + 4\text{H}_2\text{O}(\text{l})$	+0.06 V
$2\text{CO}_2(\text{g}) + 12\text{H}^+ + 12\text{e}^- \rightleftharpoons \text{CH}_3\text{CH}_2\text{OH}(\text{g}) + 3\text{H}_2\text{O}(\text{l})$	+0.08 V

which has been shown to make over 16 different products upon applied potential.^{67,68} As early as 2011, MOF-based catalysts have been reported for carbon dioxide reduction by incorporating known molecular catalysts into the linker structure.¹⁴ Driven both photo- and electrochemically, there are many examples of MOF-based carbon dioxide reduction, producing a wide range of products including carbon monoxide, formic acid, oxalic acid, ethanol, and methanol (often with significant amounts of H₂).^{69–74}

With selectivity as a major challenge in carbon dioxide reduction, it is of benefit to target reduction products that have high market value. While a full technoeconomic analysis of carbon dioxide reduction is beyond the scope of this perspective, it may be useful to consider the economic impact of specific carbon dioxide reduction products when designing selective catalysts (Figure 5). For example, although methane

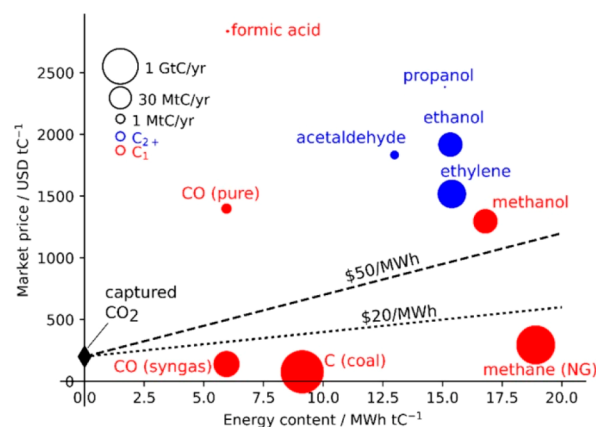


Figure 5. Comparison of market price and energy content of various CO₂ reduction products. Lines represent cost of energy from solar energy installations as an average (\$50/MWh) and record low (\$20/MWh). Reprinted with permission from ref 75. Copyright 2019 American Chemical Society.

has a high energy density per ton of carbon, the abundance of methane from other sources, like natural gas, make its overall value quite low for a primary product of carbon dioxide reduction. On the other hand, formate, methanol, or other commodity chemicals may offer smaller energy density per ton of carbon, but have vastly higher market prices, making their production from carbon dioxide reduction highly desired.^{75–77} While formate selective catalysts have been incorporated into MOFs,⁷⁸ methanol and other more complex reduction products remain a challenge to produce. Design principles learned from heterogeneous catalysts can be applied to new MOF approaches to drive methanol production or C–C bond formation. While not an exhaustive list, surface composition/adsorbates and local concentration (of H⁺ and CO) have been identified as key properties in selecting the pathway for carbon dioxide reduction to a specific product.⁷⁹ Other approaches, such as cascade catalysis, can also be employed to increase the efficiency for more complex products.⁸⁰ MOFs provide a unique platform to significantly tune each property through careful framework construction and catalyst incorporation, which may lead to excellent, selective carbon dioxide reduction catalysts.

One of the most significant steps in determining the product of carbon dioxide reduction is the formation of adsorbed species, particularly *CO onto the catalyst surface.^{75,79,81}

Bound CO can undergo further reduction to formate and methanol or dimerize with other bound species to form multicarbon products. In addition, selective adsorption of CO₂ over H⁺ is the critical component for driving carbon dioxide reduction over proton reduction. Experimental results done on heterogeneous systems have already demonstrated advantages of crystal face engineering, dopants, and heteroatoms for binding specific intermediates and directing CO₂ reduction to a desired product.⁸² While surface chemistry at bulk heterogeneous catalysts is not well understood, MOFs provide the advantage of structurally resolved nodes to serve as adsorption sites. These adsorption sites are uniform throughout the structure and can be tuned to allow for multiple binding sites within close proximity, crucial for achieving C₂₊ products. Furthermore, modification of MOF nodes through organic capping agents or metallic substitutions has gained significant interest recently.^{83–88} For example, addition of triflate groups to Zr nodes has been shown to increase the Lewis acidity of the MOF nodes, increasing the reactivity for Lewis acid driven catalysis.⁸⁹ MOF nodes can also be modified through doping to create mixed metal nodes, or through addition of single atom sites, which can tune the electron density of the MOF node.^{88,90} It may be possible to tune the binding affinity for *CO (and *H) on MOF nodes through similar modification, resulting in improved selectivity.

In addition to adsorbates, local concentrations of key reactants such as H⁺ and CO play a significant role in determining product selectivity in carbon dioxide reduction.⁹¹ For example, in other heterogeneous catalysts, boosting the local concentration of CO by combining a catalyst that is highly active for CO production with a surface with favorable CO binding and C–C bond formation has achieved great success for the production of C₂₊ products.^{79,81} Changing the concentration of reagent by changing solvents (e.g., moving to super critical CO₂ instead of atmospheric concentrations) has also been shown to change selectivity for heterogeneous CO₂ reduction catalysts.⁹² Here, the small pores of MOFs provide a unique platform for boosting local concentrations of key reactants or intermediates that may change reactivity or selectivity for a desired reaction. In fact, MOF-based catalysis for acyl transfer has demonstrated increased reactivity when loaded with a pre-concentration of specific intermediates.⁹³ Utilizing a similar approach may be the key to developing MOF-based catalysts that are highly selective for a particular CO₂ reduction product.

In addition to better understanding the different reduction pathways for CO₂, a new approach to producing complex reduction products has recently emerged. Commonly known as multistep catalysis, or cascade chemistry, this approach utilizes multiple catalysts used in series, where multielectron reduction can occur through coupled steps with a common intermediate.⁸⁰ Carbon dioxide reduction is an excellent candidate for cascade chemistry, since the straight reduction of carbon dioxide to high value products involves multiple proton-coupled electron transfer steps. Molecular examples of carbon dioxide reduction cascade chemistry have been shown to produce methanol with TON > 1.^{94,95} This approach is especially suited for MOFs, which, due to their high modularity, can incorporate multiple catalysts within close proximity to one another. Recent examples of MOF-based cascade chemistry have demonstrated the utility of this technique producing catalysts with high selectivity and long-term stability.^{96,97} In these examples, CO₂ is first reduced to

formic acid by a molecular catalyst incorporated into the MOF pores. The Lewis acidic Zr₆ nodes then convert formic acid to methyl formate before a second encapsulated catalyst is responsible for the conversion of methyl formate to methanol. In this way, the efficiency of each catalyst can be optimized (somewhat) independently, likely leading to higher yield and faster rates than a single-site approach. Not to be understated, MOFs *uniquely* provide the opportunity to easily incorporate catalysts into the linker, node, or pore to produce a material with multiple, highly selective, catalysts that work together to produce complex intermediates.

While most MOF-based approaches utilize known catalysts for incorporation, MOFs offer the potential to move beyond just heterogenization of molecular species. MOFs provide a platform to create new motifs not possible in other environments which may have enhanced catalytic properties. Molecular catalysts often rely on sterically bulky chelating ligands to prevent the formation of oligomers or metal oxide clusters. However, metal centers incorporated into the MOF structure are prevented from undergoing intermolecular deactivation pathways without the addition of more chelating ligands, opening up new species and reactivity that are inaccessible in homogeneous catalysis.⁹⁸ One example is the discovery of a series of new MOF-based hydrogenation catalysts, called MOF-Co.⁹⁸ The series, composed of Zr₆ nodes and bipyridine-derived linkers, contains coordinated (bpy)Co(THF)₂ catalysts active for the hydrogenation of a range of olefins. In solution, (Me₂bpy)Co(THF)₂ undergoes intermolecular ligand disproportionation to form Co(Me₂bpy)₂ and Co nanoparticles both inactive for hydrogenation (Figure 6). Incorporation of the Co catalyst into the MOF backbone prevents this deactivation pathway and provides highly active materials with no simple molecular analogue.

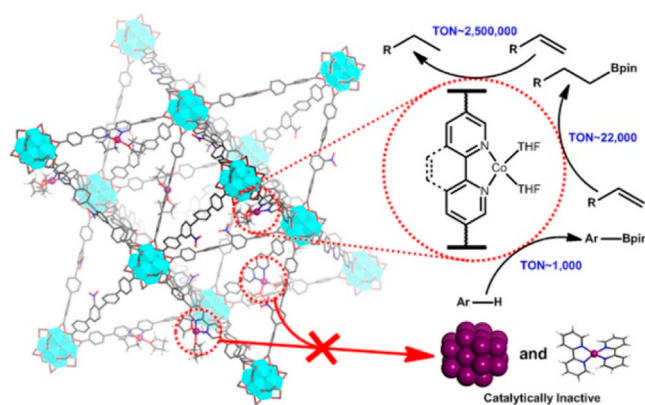


Figure 6. New MOF-based catalyst with extremely active Co sites which dimerize in solution to form inactive species. Reprinted with permission from 98. Copyright 2016 American Chemical Society.

5. INTEGRATED STUDIES

The vast majority of work that contributes to the goal of artificial photosynthesis is conducted on an isolated half-reaction (carbon dioxide reduction, water oxidation, or proton reduction). In a true artificial photosynthetic assembly, observed kinetics could be limited by mass transport, proton transport, or catalysis at any one of the active sites. Therefore, to determine the impact of systematic catalyst modifications, separation from the complete system is necessary. That said, the separation and study of a catalyst under ideal conditions do

not guarantee that the chemistry will translate to the combined approach. Combining multiple components with different rates may result in unforeseen bottlenecks that cause local buildup of H^+ , OH^- or other intermediates, unexpected side reactions, and/or photodegradation. Early examples of total MOF-driven water splitting have highlighted this potential pitfall, where careful tuning of the ratio of photosensitizers to catalysts was necessary to maximize efficiency.³⁶ The results mimic the approach in natural photosynthesis, with high concentrations of chromophores (or chlorophyll) relative to the catalytic center (or chlorophyll special pair). Under these conditions charge recombination at the special pair is minimized by thousands of light harvesters working together. These observations emphasize the need for integrated studies that combine light absorption, water oxidation, and carbon dioxide reduction. While combining all three components into a MOF or combination of MOFs remains a substantial task, initial steps can be made to remove sacrificial reagents and move toward photoelectrochemical cells.

5.1. Sacrificial Reagents. When isolating an artificial photosynthetic half-reaction, a source or sink of electrons is still required. Thus, sacrificial electron acceptors or donors (SEA/SED) are employed. Sacrificial reagents used in MOF-based catalytic H_2O oxidation or H^+/CO_2 reduction are summarized in Table 3. As the name suggests, sacrificial

Table 3. Sacrificial Reagents Used for MOF-Based Photocatalytic Reactions

Sacrificial Reagent	Catalytic Reaction	Selected Ref
TEOA (triethanolamine)	CO_2 reduction	17, 99
TEA (triethylamine)	CO_2 reduction	100
BNAH (1-benzyl-1,4-dimethyl-2,2'-bipyridine)	CO_2 reduction	99
SO_3^{2-}	CO_2 reduction	101
MeOH (methanol)	H_2 evolution	102
Na_2EDTA	H_2 evolution	103
Ascorbic acid/Ascorbate	H_2 evolution	21, 104
TEOA (triethanolamine)	H_2 evolution	105
TEA (triethylamine)	H_2 reduction	22,106
DMA (N,N' -dimethylaniline)	H_2 evolution	107, 108
Ag^+	H_2O oxidation	109
$S_2O_8^{2-}$	H_2O oxidation	110
CAN (ceric ammonium nitrate)	H_2O oxidation	14

reagents are consumed continuously in the photocatalytic reaction and are not regenerated. Thus, the reaction will be limited by the amount of sacrificial reagent. Obviously, for large scale applications this approach is unrealistic, but even beyond concerns about sustainability, the use of sacrificial reagents can complicate the reaction mechanism and obscure how the catalyst may perform in a combined approach. Additionally, sacrificial reagent choice can have a significant impact on MOF stability.

Although MOFs can achieve a wide range of chemical and thermal stability, many frameworks have a limited set of conditions in which they are stable (*vide infra*).^{111,112} However, sacrificial reagents typically have specific working conditions that may lead to poor stability of the framework or dictate the specific MOF used. For instance, TEA (pK_a 10.7) and TEOA (pK_a 7.9) will be primarily protonated when the

pH is lower than their stated pK_a value. Their ability to serve as efficient SEDs will be attenuated under such conditions. Therefore, a high pH working environment is usually necessary to achieve ideal performance of TEA and TEOA in CO_2 reduction reactions. As a result, only MOFs stable to the working conditions of the sacrificial reagent, in this case high pH, are used for CO_2 reduction. However, a fully integrated system will get electrons from H_2O oxidation and is not limited to the pH range of a sacrificial reagent. In this way, use of sacrificial reagents unnecessarily limits potential frameworks for artificial photosynthesis.

In addition to imposing new limitations, sacrificial reagents may complicate investigation of catalytic performance. In the most egregious case, the sacrificial reagent may decompose into the major product of the reaction, artificially boosting the catalytic activity. Examples of $S_2O_8^{2-}$ decomposing into O_2 for water oxidation or EDTA into oxalic and formic acid for CO_2 reduction have been previously observed.^{113–115} Less dramatically, consumed sacrificial reagents may form contaminants like nanoparticles¹⁰⁹ or dissolved species with catalytic activity¹¹⁶ that complicate isolation of the performance of the catalyst being studied. In fact, although sacrificial reagents are added to simplify a redox reaction, there are still significant questions about even the most common sacrificial reagents and their role in the reaction. Recent studies on tertiary amines for CO_2 reduction propose no less than three direct roles for TEOA in the reduction of CO_2 , significantly complicating any observed catalytic performance.^{117,118} In fact, a recent report on CO_2 reduction by MOF-545 examined the role of TEOA and found TEOA $^{\bullet}$ to be the main reducing species instead of the incorporated metalloporphyrin.¹¹⁹ In this case, formate production by metalated MOF-545 was directly caused by the sacrificial donor, rather than the previously proposed catalyst. While sacrificial reagents may be necessary in fundamental studies, new work should aim to move away from their use to more closely resemble relevant device architectures. While the combination of light sensitizer, oxidation, and reduction catalyst in a MOF-based assembly is a monumental task, moving away from sacrificial reagents toward a photoelectrochemical approach is a more manageable step.

5.2. Photoelectrochemical Cells. Photoelectrochemical cells (PECs) provide an excellent stepping stone from studying half reactions to the final goal of a fully solar powered, artificial photosynthetic array. In a PEC, two half reactions are physically separated, and coupled by an external circuit. Ion transport occurs between two electrodes in solution (or through a membrane, e.g., Nafion) while electrons transfer through the circuit. The reactions are driven by an applied potential, often lower than normally required due to the presence of a light absorber on the anode and/or cathode. For large scale solar fuel production, PECs offer significant potential since they allow for separation the anode and cathode which provides safer operating conditions and ease of product isolation.

Recently, PECs utilizing MOF-based materials for photoelectrochemical water oxidation and carbon dioxide or proton reduction have been reported.^{70,73,74,120,121} Most commonly, MOF-based PECs are created with the addition of a semiconductor as a photosensitizing layer. In this approach, MOF particles are either deposited or directly grown from a thin semiconductor layer deposited on an electrode. Examples of MOF/semiconductor composite films like HKUST-1 grown onto Cu_2O have exhibited enhanced photocurrent density,

better charge mobility, and improved semiconductor stability over the pure MOF or semiconductor film.¹²² Other materials, such as $\text{Co}_2(\text{bim})_4$ (where bim = benzimidazole) on BiVO_4 , display similar enhancements for water oxidation.¹²³ While encouraging, the field of MOF/semiconductor films is still relatively new, and significant improvement may be achievable through precise film growth, morphology control, and optimized charge transport between the MOF and semiconductor layers.

6. STABILITY

While MOFs as a whole exhibit a wide range of stability, most MOF structures are stable only under specific conditions. Take, for example, MOF-5 (or IRMOF-1) whose surface area has been shown to decrease from $3800 \text{ m}^2/\text{g}$ to $570 \text{ m}^2/\text{g}$ simply by exposure to humid environments.^{124,125} Artificial photosynthetic chemistry must take place in an aqueous environment, which effectively eliminates MOFs like MOF-5, and other structures that are unstable in aqueous media. While certain MOFs are more stable to the addition of water, like the UiO series, they easily degrade at high pH or in the presence of phosphate buffers.¹¹¹ Clearly, understanding MOF degradation pathways is crucial to developing materials with long-term stability to the required catalytic conditions. Luckily, fundamental principles such as hard–soft acid–base theory can be used to predict node–ligand interactions. For example, the instability of MOF-5 can be attributed to the relatively weak metal–linker bond formed between a soft acid (Zn^{2+}) and a hard base (terephthalic acid).¹²⁶ The same ligand, when connected to a hard Zr^{4+} node, forms a highly chemically stable MOF, UiO-66. Although MOFs contain a diverse selection of nodes and linkers, degradation of MOFs can often be understood through the strength of the metal–ligand bond. When species are present in solution that bind more strongly to the node than the organic linker, MOF degradation will occur.^{126–128} It should also be noted that even strong metal–ligand bonds are not static and all MOF structures, even structures traditionally thought to be highly stable such as UiO-66 and MIL-125, are in a constant state of dynamic bonding, which may play a critical role in observed MOF properties, specifically catalysis.⁴³

Linker modifications can also significantly alter MOF stability. Some structural modifications such as linker elongation can result in drastically reduced stabilities due to increased flexibility with linker length. For example, the extended linker in UiO-67 shows decreased stability compared to the smaller UiO-66.¹²⁹ Further extending the linker to four rings results in a framework that is not stable to solvent removal.¹³ Other factors such as torsional distortion and linker strain may further complicate the question of stability. Linker modification with functional groups can result in modified stability; for example, UiO-66- NO_2 displays higher stability in aqueous environments compared to native UiO-66.¹¹¹ The changes in stability from linker modification can be difficult to predict. The electron withdrawing $-\text{NO}_2$ group would not conventionally suggest improved stability over native UiO-66. It was hypothesized that the ligand modification resulted in fewer structural defects (missing linker/missing node) and the increased stability was a result of these properties. Taken together, the ability to predict stability *a priori* is complex and many factors need to be considered.

In photoelectrochemical approaches a new challenge, namely the impact of applied potential on stability, is

introduced. Applying potentials sufficient to drive electrochemical reactivity may result in structural changes at MOF nodes or redox active linkers. Many redox-active molecular complexes undergo geometry changes during catalytic cycling. For instance, tetrahedral Co^{II} complexes can yield octahedral compounds upon oxidation. When this occurs at a MOF node, the geometry change may result in degradation or transformation of the framework. As an example, HKUST-1 ($\text{Cu}_3(\text{BTC})_2$, BTC = 1,3,5-benzene-tricarboxylic acid) was thought to be active for CO_2 reduction with comparable rates of other molecular Cu-based catalysts. However, HKUST-1 shows irreversible electrochemistry and postcatalytic studies with EXAFS, PXRD, and SEM suggest loss of MOF structure and formation of Cu metal nanoparticles (Figure 7).¹³⁰ Similar

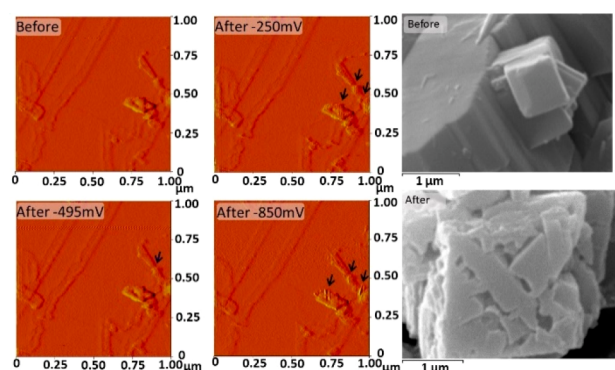


Figure 7. AFM and SEM of an HKUST-1 modified electrode after an applied potential. Arrows and degradation due to formation of Cu nanoparticles. Adapted with permission from ref 130. Copyright 2007 American Chemical Society.

degradation of a Co-based MOF, CoPIZA, which contains trinuclear Co nodes connected by a cobalt containing porphyrin linker, was observed upon reduction to the +1 oxidation state.³⁴

In addition to framework stability, catalytically loaded MOFs have other, unique stability concerns to consider. For loaded MOF structures, catalytic leaching cannot be detected using conventional MOF characterization techniques like powder X-ray diffraction (PXRD). For example, $\text{Re}(\text{bpy})(\text{CO})_3\text{X}$ (where bpy = 2,2'-bipyridine and X is a halide) is a known CO_2 reduction catalyst that suffers from deactivation by photodissociation of the Re moiety from the bipyridine group. When $\text{Re}(\text{bpy})(\text{CO})_3\text{X}$ was incorporated into UiO-67, Wang et al. observed catalytic activity for two catalytic cycles before no additional product is detected.¹⁴ The loss of catalytic activity was attributed to leaching of near 50% of the incorporated Re catalyst, as observed by inductively coupled plasma mass spectrometry (ICP-MS). PXRD of the framework after catalysis showed no sign of degradation, indicating that the MOF structure was retained, while the molecular Re catalyst dissociated from the MOF backbone.

Due to the complex nature of artificial photosynthesis, and MOFs in general, there are many stability concerns to be considered without a “one size fits all” solution. This is not to say that MOFs are unstable, but rather it is critical to be selective with framework choice for each environment and application it will be used for. Few materials are infinitely stable, but proper selection (or postsynthetic modifications and additions) can dramatically improve MOF stability for a given reaction. Additionally, careful consideration should be given to

the role of the metal node, particularly in redox reactions. Utilizing the MOF node as a redox hopping center and as a structural pillar often leads to instability due to geometry changes during redox changes. Separating functions, structural or chemical, may provide additional stability benefits.

Considering the intricacies of MOF stability, general guidelines should be followed to confirm stability during catalysis. While these guidelines may not be possible for every MOF, they can be applied to most structures to gain a better understanding of how MOFs compare to other catalytic assemblies in terms of stability. The following should be conducted pre- and post-catalysis:

1. Powder X-ray Diffraction (PXRD)
2. Scanning Electron Microscopy (SEM)
3. ICP-MS, and/or ^1H NMR
4. Surface Area Analysis

Perhaps the most important of all postcatalytic characterization is PXRD. Due to the highly crystalline nature of MOFs and their characteristic diffraction peaks, PXRD is an excellent tool to monitor structural changes before and after catalysis. Diffraction patterns should show consistent peak positions and relative peak intensities to provide support for long-range structural stability during catalysis. If peak positions or relative intensities change postcatalysis, further study should be done to determine the identity and stability of the new MOF phase. Although PXRD cannot be used to identify structural changes that arise from amorphous material, it remains a powerful technique to confirm the structural integrity of the MOF throughout the catalytic process. Ideally, if the framework has been previously synthesized (or is isostructural to a known MOF), quantitative comparison of the experimental PXRD to the unit cell of the predicted pattern should be done to confirm exact structural identity. If available, temperature dependent PXRD studies may be helpful to show crystallinity at desired reaction temperatures. While bulk thermal stability can be measured by thermogravimetric analysis, temperature dependent PXRD may reveal structural changes at elevated temperatures. In some cases, these changes can occur before the thermal decomposition temperature measured by TGA.^{131,132} These structural changes may be caused by loss of structured solvent, gradual removal of linkers causing new defect sites, or even changes in the MOF node.

While PXRD is a powerful way to look for structural changes in the MOF, it can only examine the material left behind, so any MOF that degraded into its molecular constituents (or other byproducts) is not detected by this technique. Combining PXRD with a visualization technique such as SEM or TEM provides a better understanding of potential postcatalytic degradation. Imaging techniques like SEM can also be combined with energy dispersive X-ray spectroscopy (EDS) to examine MOF composition and catalyst distribution. One study which highlights the need for TEM/PXRD studies is a paper by Shi et al., where a new MOF was synthesized, Cu-X-bpy ($X = \text{halide}$), for light-driven hydrogen evolution.²² PXRD showed excellent crystallinity in a variety of solvents and temperatures up to 250 °C, but further investigation with TEM showed formation of Cu nanoparticles on the MOF surface caused by photoreduction of the Cu nodes (Figure 8). Even if the remaining material is crystalline by PXRD, it is clear the framework partially degrades during catalysis. As a result, it is difficult to unambiguously attribute catalytic properties to the framework and not the nanoparticles that are formed.

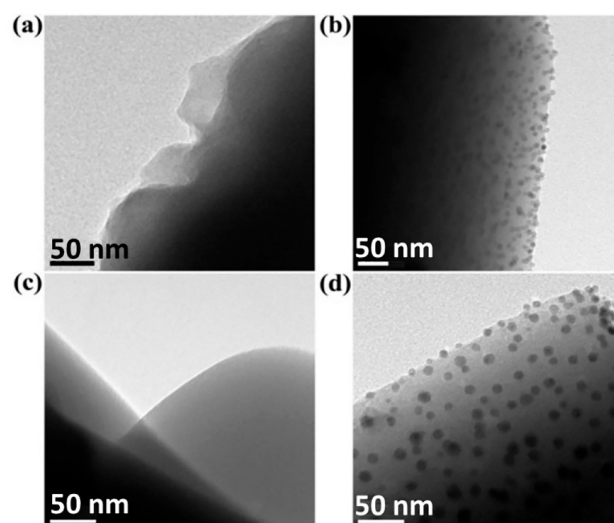


Figure 8. TEM images of Cu-X-bpy MOFs showing formation of nanoparticles. Adapted with permission from ref 22. Copyright 2017, John Wiley and Sons.

To quantify catalyst leaching, composition studies can be done by several different analytical techniques depending on the framework and catalyst in question. ICP-MS, ^1H NMR, FT-IR, and diffuse reflectance are all analytical techniques that can be used to identify potential changes in MOF composition after catalysis. Careful consideration of the MOF should be used when selecting a technique. Complete digestion of the sample (in the case of ICP-MS, or ^1H NMR) is critical to ensure reproducible results and may require harsh reagents such as HF for stable MOFs. Each technique can be used on the MOF and the supernatant, where degradation products can be identified. Some materials, such as UiO-66-NH_2 have previously been considered stable photocatalysts for carbon dioxide reduction under basic conditions. However, after filtering the reaction solution to remove MOF, ICP detects small traces of leached zirconium (0.1–0.8%). When this filtered solution is charged with carbon dioxide the dissolved Zr can convert carbon dioxide to formate with a higher TON than the solid MOF particles.¹¹⁶ In this case, it is difficult to determine if the catalytic activity is due to the MOF or dissolved Zr species formed as the MOF degrades.

Another characterization technique that may be useful for determining catalytic stability is gas sorption measurements to determine surface area. Surface area analysis can give valuable insight into the structural integrity of the framework and can be used as a direct measure of framework collapse. Internal surface area and pore size distribution should be similar before and after catalysis if the framework is stable under reaction conditions. However, it is important to note that small changes in conditions can result in a significant change in the observed surface areas. Care should be taken that samples pre- and postcatalysis are properly activated for direct comparison. For new frameworks, computational methods can be used to model expected surface areas. These calculations, although not exact, should provide a good estimate of the internal surface area as long as the structure follows BET theory.¹³³ Additionally, it is critically important to pair surface area measurements with PXRD as structural changes as a result of gas sorption are prevalent.

In addition to the techniques listed above, there are a number of extremely powerful techniques that have recently

been utilized to study MOF chemistry like EXAFS, XANES, and difference-electron-density measurements among others. Unfortunately, many of these powerful analyses require the use of synchrotron facilities and cannot be performed as part of routine analysis. Our recommendations here are not meant to be an exhaustive list of MOF characterization techniques, rather a set of standard measurements that can be achieved in most academic laboratories. If other, more powerful techniques are available they should most certainly be used.

7. CONCLUSION

Over the past several years, interest in MOFs for artificial photosynthesis has grown significantly. The potential of functional MOFs has been known, but recent advancements in the field have brought MOF systems closer to realizing that potential and have offered valuable insights critical to future design. In this perspective, we have proposed four key areas for further investigation: mass and charge transport, catalytic selectivity, integrated studies, and stability.

Since their first use in catalytic reactions, two of the major benefits of MOFs have been the permanent porosity and high internal surface areas. However, due to the small pore sizes, even in “large pore MOFs”, diffusion has been a significant challenge in MOF-based reactions. While large diameter pores may improve mass transport into the framework, diffusion rates are still orders of magnitude slower than bulk solution phase.⁴⁴ Understanding the nature of structured solvent and solvent–MOF interactions may be critical to better understanding confined diffusion within MOF pores. In addition to mass transport, ion and proton diffusion is likely critical for industrial applications, which may be driven (partially) electrochemically and require directed transport of protons from the anode to the cathode. Matching the rate of proton transport with the rate of catalysis will be critical to avoid a dramatic increase of local pH at catalytic sites.³⁶

For an artificial photosynthetic array to be practically viable, it must function as a catalyst that is selective for a specific and desired product. Formate, methanol, and C₂₊ products are all high-value chemicals that should be targeted in CO₂ reduction.⁷⁶ MOFs have significant potential to be highly selective CO₂ reduction catalysts, even for traditionally difficult products. The repeating structures offer uniform, well-defined reaction and absorption sites with significant opportunities for tuning. Metal substitution, or functional group binding, can drastically tune the adsorption energies of MOF nodes to be highly selective for *CO over *H, a critical component for CO₂ reduction. Because MOFs offer multiple areas for catalyst incorporation, multifunctional MOFs may be the key to producing complex products. Incorporation of several catalysts that can produce intermediates near other catalysts could offer high levels of selectivity not possible in other heterogeneous catalysts. Finally, capitalizing on unique 3D structure of MOFs—node and linker—may lead to distinctive catalytic performance not possible in simple molecular species.

Early work in MOF-based artificial photosynthesis has been limited to a single component such as light absorption, H₂O oxidation, or CO₂ reduction. However, the next frontier is moving beyond from isolated half-reactions toward coupling individual components in a full MOF approach. Some recent examples of total water splitting in MOFs demonstrate challenges that are not seen when studying half-reactions.³⁶ In a half-reaction, experimental conditions are used so that the reaction under investigation is the limiting step. In a fully

combined approach, however, the overall efficiency will be limited by the slowest step. Mismatch in catalytic or diffusion rates may lead to a buildup of intermediates and reduction in overall efficiency. Additionally, while sacrificial reagents claim to simplify the reaction, they may act in unintended ways to complicate it. Moving toward PECs allows for the coupling of MOF components into an integrated array to better understand limitations of the MOF-based approach.^{37,38} That said, PEC approaches introduce new challenges such as understanding MOF film growth, morphology, and charge transport across interfaces between MOFs and supports.

Finally, as the complexity of the framework increases, so does the range of characterization that should be applied to the active material to fully understand the mechanisms taking place and the limitations of new materials. X-ray diffraction alone cannot determine the stability of a catalyst loaded framework. Other techniques such as SEM, ICP/¹H NMR, and surface area analysis should be done pre- and postcatalysis (when possible) to confirm the stability of the material, and also to rule out inflated activity due to catalytic leaching, or formation of other active species.¹¹⁶ Deep understanding of MOF stability during catalysis is critical for developing artificial photosynthetic arrays with an eye toward translation to technology. MOFs are a still relatively new class of materials, and early work has shown significant promise for complex applications such as artificial photosynthesis. Tackling the challenges outlined above will be key to advancing closer to a fully integrated MOF-based artificial photosynthetic assembly.

AUTHOR INFORMATION

Corresponding Author

Amanda J. Morris – Department of Chemistry, Virginia Polytechnic Institute and State University, Blacksburg, Virginia 24061, United States; orcid.org/0000-0002-3512-0366; Email: ajmorris@vt.edu

Authors

Bradley Gibbons – Department of Chemistry, Virginia Polytechnic Institute and State University, Blacksburg, Virginia 24061, United States; orcid.org/0000-0003-2699-3621

Meng Cai – Department of Chemistry, Virginia Polytechnic Institute and State University, Blacksburg, Virginia 24061, United States

Complete contact information is available at: <https://pubs.acs.org/10.1021/jacs.2c04144>

Notes

The authors declare no competing financial interest.

ACKNOWLEDGMENTS

This paper is adapted from a dissertation by the first author (B.G.). This material is based upon work supported by the U.S. Department of Energy, Office of Science, Office of Basic Energy Sciences, under Award DE-SC0012446.

REFERENCES

- (1) Ye, S.; Ding, C.; Liu, M.; Wang, A.; Huang, Q.; Li, C. Water Oxidation Catalysts for Artificial Photosynthesis. *Adv. Mater.* **2019**, *31* (50), 1902069.
- (2) Wang, Y.; Suzuki, H.; Xie, J.; Tomita, O.; Martin, D. J.; Higashi, M.; Kong, D.; Abe, R.; Tang, J. Mimicking Natural Photosynthesis:

Solar to Renewable H₂ Fuel Synthesis by Z-Scheme Water Splitting Systems. *Chem. Rev.* **2018**, *118* (10), 5201–5241.

(3) Bullock, J.; Wan, Y.; Xu, Z.; Essig, S.; Hettick, M.; Wang, H.; Ji, W.; Boccard, M.; Cuevas, A.; Ballif, C.; Javey, A. Stable Dopant-Free Asymmetric Heterocontact Silicon Solar Cells with Efficiencies above 20%. *ACS Energy Lett.* **2018**, *3* (3), 508–513.

(4) Brennaman, M. K.; Dillon, R. J.; Alibabaei, L.; Gish, M. K.; Dares, C. J.; Ashford, D. L.; House, R. L.; Meyer, G. J.; Papanikolas, J. M.; Meyer, T. J. Finding the Way to Solar Fuels with Dye-Sensitized Photoelectrosynthesis Cells. *J. Am. Chem. Soc.* **2016**, *138* (40), 13085–13102.

(5) Cheng, W. H.; Richter, M. H.; May, M. M.; Ohlmann, J.; Lackner, D.; Dimroth, F.; Hannappel, T.; Atwater, H. A.; Lewerenz, H. J. Monolithic Photoelectrochemical Device for Direct Water Splitting with 19% Efficiency. *ACS Energy Lett.* **2018**, *3* (8), 1795–1800.

(6) Zhang, T.; Lin, W. Metal-Organic Frameworks for Artificial Photosynthesis and Photocatalysis. *Chem. Soc. Rev.* **2014**, *43* (16), 5982–5993.

(7) Johnson, B. A.; Bhunia, A.; Ott, S. Electrocatalytic Water Oxidation by a Molecular Catalyst Incorporated into a Metal-Organic Framework Thin Film. *Dalt. Trans.* **2017**, *46* (5), 1382–1388.

(8) Lin, S.; Pineda-Galvan, Y.; Maza, W. A.; Epley, C. C.; Zhu, J.; Kessinger, M. C.; Pushkar, Y.; Morris, A. J. Electrochemical Water Oxidation by a Catalyst-Modified Metal-Organic Framework Thin Film. *ChemSusChem* **2017**, *10*, 514–522.

(9) Lin, S.; Ravari, A. K.; Zhu, J.; Usov, P. M.; Cai, M.; Ahrenholtz, S. R.; Pushkar, Y.; Morris, A. J. Insight into Metal-Organic Framework Reactivity: Chemical Water Oxidation Catalyzed by a [Ru(Tpy)-(Dcbpy)(OH₂)]²⁺-Modified UiO-67. *ChemSusChem* **2018**, *11* (2), 464–471.

(10) Lu, X. F.; Liao, P. Q.; Wang, J. W.; Wu, J. X.; Chen, X. W.; He, C. T.; Zhang, J. P.; Li, G. R.; Chen, X. M. An Alkaline-Stable, Metal Hydroxide Mimicking Metal-Organic Framework for Efficient Electrocatalytic Oxygen Evolution. *J. Am. Chem. Soc.* **2016**, *138* (27), 8336–8339.

(11) Ma, J. P.; Wang, S. Q.; Zhao, C. W.; Yu, Y.; Dong, Y. B. Cu(II)-Metal-Organic Framework with Open Coordination Metal Sites for Low Temperature Thermochemical Water Oxidation. *Chem. Mater.* **2015**, *27* (11), 3805–3808.

(12) Meyer, K.; Ranocchiari, M.; Van Bokhoven, J. A. Metal Organic Frameworks for Photo-Catalytic Water Splitting. *Energy Environ. Sci.* **2015**, *8* (7), 1923–1937.

(13) Wang, C.; Wang, J. L.; Lin, W. Elucidating Molecular Iridium Water Oxidation Catalysts Using Metal-Organic Frameworks: A Comprehensive Structural, Catalytic, Spectroscopic, and Kinetic Study. *J. Am. Chem. Soc.* **2012**, *134* (48), 19895–19908.

(14) Wang, C.; Xie, Z.; DeKrafft, K. E.; Lin, W. Doping Metal Organic Frameworks for Water Oxidation, Carbon Dioxide Reduction, and Organic Photocatalysis. *J. Am. Chem. Soc.* **2011**, *133*, 13445–13454.

(15) Xu, H. Q.; Hu, J.; Wang, D.; Li, Z.; Zhang, Q.; Luo, Y.; Yu, S. H.; Jiang, H. L. Visible-Light Photoreduction of CO₂ in a Metal-Organic Framework: Boosting Electron-Hole Separation via Electron Trap States. *J. Am. Chem. Soc.* **2015**, *137* (42), 13440–13443.

(16) Wang, D.; Huang, R.; Liu, W.; Sun, D.; Li, Z. Fe-Based MOFs for Photocatalytic CO₂ Reduction: Role of Coordination Unsaturated Sites and Dual Excitation Pathways. *ACS Catal.* **2014**, *4* (12), 4254–4260.

(17) Elcheikh Mahmoud, M.; Audi, H.; Assoud, A.; Ghaddar, T. H.; Hmadeh, M. Metal-Organic Framework Photocatalyst Incorporating Bis(4'-(4-Carboxyphenyl)-Terpyridine)Ruthenium(II) for Visible-Light-Driven Carbon Dioxide Reduction. *J. Am. Chem. Soc.* **2019**, *141* (17), 7115–7121.

(18) Luo, Y. H.; Dong, L. Z.; Liu, J.; Li, S. L.; Lan, Y. Q. From Molecular Metal Complex to Metal-Organic Framework: The CO₂ Reduction Photocatalysts with Clear and Tunable Structure. *Coord. Chem. Rev.* **2019**, *390*, 86–126.

(19) Feng, X.; Pi, Y.; Song, Y.; Brzezinski, C.; Xu, Z.; Li, Z.; Lin, W. Metal-Organic Frameworks Significantly Enhance Photocatalytic Hydrogen Evolution and CO₂ Reduction with Earth-Abundant Copper Photosensitizers. *J. Am. Chem. Soc.* **2020**, *142* (2), 690–695.

(20) Hou, C. C.; Li, T. T.; Cao, S.; Chen, Y.; Fu, W. F. Incorporation of a [Ru(Dcbpy)(Bpy)₂]²⁺ Photosensitizer and a Pt(Dcbpy)Cl₂ Catalyst into Metal-Organic Frameworks for Photocatalytic Hydrogen Evolution from Aqueous Solution. *J. Mater. Chem. A* **2015**, *3* (19), 10386–10394.

(21) Guo, W.; Lv, H.; Chen, Z.; Sullivan, K. P.; Lauinger, S. M.; Chi, Y.; Sumliner, J. M.; Lian, T.; Hill, C. L. Self-Assembly of Polyoxometalates, Pt Nanoparticles and Metal-Organic Frameworks into a Hybrid Material for Synergistic Hydrogen Evolution. *J. Mater. Chem. A* **2016**, *4* (16), 5952–5957.

(22) Shi, D.; Zheng, R.; Sun, M.; Cao, X.; Sun, C.; Cui, C. Semiconductive Copper (I)-Organic Frameworks for Efficient Light-Driven Hydrogen Generation Without Additional Photosensitizers and Cocatalysts. *Angewandte* **2017**, *475004*, 14637–14641.

(23) Zhang, Q.; Zhang, C.; Cao, L.; Wang, Z.; An, B.; Lin, Z.; Huang, R.; Zhang, Z.; Wang, C.; Lin, W. Förster Energy Transport in Metal-Organic Frameworks Is beyond Step-by-Step Hopping. *J. Am. Chem. Soc.* **2016**, *138* (16), 5308–5315.

(24) Lee, C. Y.; Farha, O. K.; Hong, B. J.; Sarjeant, A. A.; Nguyen, S. T.; Hupp, J. T. Light-Harvesting Metal-Organic Frameworks (MOFs): Efficient Strut-to-Strut Energy Transfer in Bodipy and Porphyrin-Based MOFs. *J. Am. Chem. Soc.* **2011**, *133* (40), 15858–15861.

(25) Son, H. J.; Jin, S.; Patwardhan, S.; Wezenberg, S. J.; Jeong, N. C.; So, M.; Wilmer, C. E.; Sarjeant, A. A.; Schatz, G. C.; Snurr, R. Q.; Farha, O. K.; Wiederrecht, G. P.; Hupp, J. T. Light-Harvesting and Ultrafast Energy Migration in Porphyrin-Based Metal-Organic Frameworks. *J. Am. Chem. Soc.* **2013**, *135* (2), 862–869.

(26) Park, H. J.; So, M. C.; Gosztoła, D.; Wiederrecht, G. P.; Emery, J. D.; Martinson, A. B. F.; Er, S.; Wilmer, C. E.; Vermeulen, N. A.; Aspuru-Guzik, A.; Stoddart, J. F.; Farha, O. K.; Hupp, J. T. Layer-by-Layer Assembled Films of Perylene Diimide- and Squaraine-Containing Metal-Organic Framework-like Materials: Solar Energy Capture and Directional Energy Transfer. *ACS Appl. Mater. Interfaces* **2016**, *8* (38), 24983–24988.

(27) Lin, S.; Cairnie, D. R.; Chakraborty, A.; Cai, M.; Morris, A. J. Photoelectrochemical Alcohol Oxidation by Mixed-Linker Metal-Organic Frameworks. *Faraday Discuss.* **2020**, 371–383.

(28) Maza, W. A.; Padilla, R.; Morris, A. J. Concentration Dependent Dimensionality of Resonance Energy Transfer in a Postsynthetically Doped Morphologically Homologous Analogue of UiO-67 MOF with a Ruthenium(II) Polypyridyl Complex. *J. Am. Chem. Soc.* **2015**, *137* (25), 8161–8168.

(29) Maza, W. A.; Haring, A. J.; Ahrenholtz, S. R.; Epley, C. C.; Lin, S. Y.; Morris, A. J. Ruthenium(II)-Polypyridyl Zirconium(IV) Metal-Organic Frameworks as a New Class of Sensitized Solar Cells. *Chem. Sci.* **2016**, *7* (1), 719–727.

(30) Chakraborty, A.; Ilic, S.; Cai, M.; Gibbons, B. J.; Yang, X.; Slamowitz, C. C.; Morris, A. J. Role of Spin-Orbit Coupling in Long Range Energy Transfer in Metal-Organic Frameworks. *J. Am. Chem. Soc.* **2020**, *142* (48), 20434–20443.

(31) Sun, L.; Campbell, M. G.; Dincă, M. Electrically Conductive Porous Metal-Organic Frameworks. *Angew. Chemie - Int. Ed.* **2016**, *55* (11), 3566–3579.

(32) Leong, C. F.; Usov, P. M.; D'Alessandro, D. M. Intrinsically Conducting Metal-Organic Frameworks. *MRS Bull.* **2016**, *41* (11), 858–864.

(33) Hod, I.; Farha, O. K.; Hupp, J. T. Modulating the Rate of Charge Transport in a Metal-Organic Framework Thin Film Using Host:Guest Chemistry. *Chem. Commun.* **2016**, *52* (8), 1705–1708.

(34) Ahrenholtz, S. R.; Epley, C. C.; Morris, A. J. Solvothermal Preparation of an Electrocatalytic Metalloporphyrin MOF Thin Film and Its Redox Hopping Charge-Transfer Mechanism. *J. Am. Chem. Soc.* **2014**, *136* (6), 2464–2472.

- (35) Kornienko, N.; Zhao, Y.; Kley, C. S.; Zhu, C.; Kim, D.; Lin, S.; Chang, C. J.; Yaghi, O. M.; Yang, P. Metal-Organic Frameworks for Electrochemical Reduction of Carbon Dioxide. *J. Am. Chem. Soc.* **2015**, *137* (44), 14129–14135.
- (36) Hu, H.; Wang, Z.; Cao, L.; Zeng, L.; Zhang, C.; Lin, W.; Wang, C. Metal-Organic Frameworks Embedded in a Liposome Facilitate Overall Photocatalytic Water Splitting. *Nat. Chem.* **2021**, 1–9.
- (37) Duan, J.; Chen, S.; Zhao, C. Ultrathin Metal-Organic Framework Array for Efficient Electrochemical Water Splitting. *Nat. Commun.* **2017**, *8*, 1–7.
- (38) Raja, D. S.; Chuah, X.; Lu, S. In Situ Grown Bimetallic MOF-Based Composite as Highly Efficient Bifunctional Electrocatalyst for Overall Water Splitting with Ultrastability at High Current Densities. *Adv. Energy Mater.* **2018**, *8*, 1801065.
- (39) Hönicke, I. M.; Senkowska, I.; Bon, V.; Baburin, I. A.; Bönisch, N.; Raschke, S.; Evans, J. D.; Kaskel, S. Balancing Mechanical Stability and Ultrahigh Porosity in Crystalline Framework Materials. *Angew. Chemie - Int. Ed.* **2018**, *57* (42), 13780–13783.
- (40) Rothenberg, G. Heterogeneous Catalysis. In *Catalysis: Concepts and Green Applications*; Wiley Online Books: 2008; pp 127–187. DOI: 10.1002/9783527621866.ch4.
- (41) Wang, C.; Lin, W. Diffusion-Controlled Luminescence Quenching in Metal-Organic Frameworks. *J. Am. Chem. Soc.* **2011**, *133* (12), 4232–4235.
- (42) Choi, H. J.; Suh, M. P. Dynamic and Redox Active Pillared Bilayer Open Framework: Single-Crystal-to-Single-Crystal Transformations upon Guest Removal, Guest Exchange, and Framework Oxidation. *J. Am. Chem. Soc.* **2004**, *126* (48), 15844–15851.
- (43) Andreeva, A. B.; Le, K. N.; Chen, L.; Kellman, M. E.; Hendon, C. H.; Brozek, C. K.; Hendon, C. H. Soft Mode Metal-Linker Dynamics in Carboxylate MOFs Evidenced by Variable-Temperature Infrared Spectroscopy. *J. Am. Chem. Soc.* **2020**, *142* (45), 19291–19299.
- (44) Cai, M.; Loague, Q.; Morris, A. J. Design Rules for Efficient Charge Transfer in Metal-Organic Framework Films: The Pore Size Effect. *J. Phys. Chem. Lett.* **2020**, *11* (3), 702–709.
- (45) Wang, R.; Bukowski, B. C.; Duan, J.; Sui, J.; Snurr, R. Q.; Hupp, J. T. Art of Architecture: Efficient Transport through Solvent-Filled Metal-Organic Frameworks Regulated by Topology. *Chem. Mater.* **2021**, *33* (17), 6832–6840.
- (46) Wang, R.; Bukowski, B. C.; Duan, J.; Sheridan, T. R.; Atilgan, A.; Zhang, K.; Snurr, R. Q.; Hupp, J. T. Investigating the Process and Mechanism of Molecular Transport within a Representative Solvent-Filled Metal-Organic Framework. *Langmuir* **2020**, *36*, 10853–10859.
- (47) Rieth, A. J.; Hunter, K. M.; Dincă, M.; Paesani, F. Hydrogen Bonding Structure of Confined Water Templated by a Metal-Organic Framework with Open Metal Sites. *Nat. Commun.* **2019**, *10* (1), 1–7.
- (48) Sharp, C. H.; Bukowski, B. C.; Li, H.; Johnson, E. M.; Ilic, S.; Morris, A. J.; Gersappe, D.; Snurr, R. Q.; Morris, J. R. Nanoconfinement and Mass Transport in Metal-Organic Frameworks. *Chem. Soc. Rev.* **2021**, *50* (20), 11530–11558.
- (49) Lim, D. W.; Kitagawa, H. Proton Transport in Metal-Organic Frameworks. *Chem. Rev.* **2020**, *120* (16), 8416–8467.
- (50) Xiang, F.; Chen, S.; Zheng, S.; Yang, Y.; Huang, J.; Lin, Q.; Wang, L.; Xiang, S.; Zhang, Z. Anhydrous Proton Conduction in Crystalline Porous Materials with a Wide Working Temperature Range. *ACS Appl. Mater. Interfaces* **2021**, *13* (35), 41363–41371.
- (51) Nguyen, N. T. T.; Furukawa, H.; Gándara, F.; Trickett, C. A.; Jeong, H. M.; Cordova, K. E.; Yaghi, O. M. Three-Dimensional Metal-Catecholate Frameworks and Their Ultrahigh Proton Conductivity. *J. Am. Chem. Soc.* **2015**, *137* (49), 15394–15397.
- (52) Tang, Q.; Liu, Y.; Liu, S.; He, D.; Miao, J.; Wang, X.; Yang, G.; Shi, Z.; Zheng, Z. High Proton Conduction at above 100°C Mediated by Hydrogen Bonding in a Lanthanide Metal-Organic Framework. *J. Am. Chem. Soc.* **2014**, *136* (35), 12444–12449.
- (53) Yang, F.; Huang, H.; Wang, X.; Li, F.; Gong, Y.; Zhong, C.; Li, J. R. Proton Conductivities in Functionalized UiO-66: Tuned Properties, Thermogravimetry Mass, and Molecular Simulation Analyses. *Cryst. Growth Des.* **2015**, *15* (12), 5827–5833.
- (54) Wang, S.; Wahiduzzaman, M.; Davis, L.; Tissot, A.; Shepard, W.; Marrot, J.; Martineau-Corcos, C.; Hamdane, D.; Maurin, G.; Devautour-Vinot, S.; Serre, C. A Robust Zirconium Amino Acid Metal-Organic Framework for Proton Conduction. *Nat. Commun.* **2018**, *9* (1), 1–8.
- (55) Liu, S. J.; Cao, C.; Yang, F.; Yu, M. H.; Yao, S. L.; Zheng, T. F.; He, W. W.; Zhao, H. X.; Hu, T. L.; Bu, X. H. High Proton Conduction in Two CoII and MnII Anionic Metal-Organic Frameworks Derived from 1,3,5-Benzenetricarboxylic Acid. *Cryst. Growth Des.* **2016**, *16* (12), 6776–6780.
- (56) Jeong, N. C.; Samanta, B.; Lee, C. Y.; Farha, O. K.; Hupp, J. T. Coordination-Chemistry Control of Proton Conductivity in the Ionic Metal-Organic Framework Material HKUST-1. *J. Am. Chem. Soc.* **2012**, *134* (1), 51–54.
- (57) Lim, D. W.; Sadakiyo, M.; Kitagawa, H. Proton Transfer in Hydrogen-Bonded Degenerate Systems of Water and Ammonia in Metal-Organic Frameworks. *Chem. Sci.* **2019**, *10* (1), 16–33.
- (58) Bureekaew, S.; Horike, S.; Higuchi, M.; Mizuno, M.; Kawamura, T.; Tanaka, D.; Yanai, N.; Kitagawa, S. One-Dimensional Imidazole Aggregate in Aluminium Porous Coordination Polymers with High Proton Conductivity. *Nat. Mater.* **2009**, *8* (10), 831–836.
- (59) Sharma, A.; Lim, J.; Jeong, S.; Won, S.; Seong, J.; Lee, S.; Kim, Y. S.; Baek, S. Bin; Lah, M. S. Superprotonic Conductivity of MOF-808 Achieved by Controlling the Binding Mode of Grafted Sulfamate. *Angew. Chemie Int. Ed.* **2021**, *60* (26), 14334–14338.
- (60) Zhang, K.; Wen, G. H.; Yang, X. J.; Lim, D. W.; Bao, S. S.; Donoshita, M.; Wu, L. Q.; Kitagawa, H.; Zheng, L. M. Anhydrous Superprotonic Conductivity of a Uranyl-Based MOF from Ambient Temperature to 110°C. *ACS Mater. Lett.* **2021**, *3* (6), 744–751.
- (61) Gupta, A.; Goswami, S.; Elahi, S. M.; Konar, S. Role of Framework-Carrier Interactions in Proton-Conducting Crystalline Porous Materials. *Cryst. Growth Des.* **2021**, *21* (3), 1378–1388.
- (62) Ye, Y.; Guo, W.; Wang, L.; Li, Z.; Song, Z.; Chen, J.; Zhang, Z.; Xiang, S.; Chen, B. Straightforward Loading of Imidazole Molecules into Metal-Organic Framework for High Proton Conduction. *J. Am. Chem. Soc.* **2017**, *139* (44), 15604–15607.
- (63) Zhang, J.; Zhang, R.; Liu, Y.; Kong, Y.-R.; Luo, H.-B.; Zou, Y.; Zhai, L.; Ren, X.-M. Acidic Groups Functionalized Carbon Dots Capping Channels of a Proton Conductive Metal-Organic Framework by Coordination Bonds to Improve the Water-Retention Capacity and Boost Proton Conduction. *ACS Appl. Mater. Interfaces* **2021**, *13* (50), 60084–60091.
- (64) Lin, S.; Usov, P. M.; Morris, A. J. The Role of Redox Hopping in Metal-Organic Framework Electrocatalysis. *Chem. Commun.* **2018**, *54* (51), 6965–6974.
- (65) Celis-Salazar, P. J.; Cai, M.; Cucinell, C. A.; Ahrenholtz, S. R.; Epley, C. C.; Usov, P. M.; Morris, A. J. Independent Quantification of Electron and Ion Diffusion in Metallocene-Doped Metal-Organic Frameworks Thin Films. *J. Am. Chem. Soc.* **2019**, *141* (30), 11947–11953.
- (66) Bard, A. J.; Faulkner, L. R. *Electrochemical Methods*, 2nd ed.; John Wiley & Sons, Ltd: 2001. DOI: 10.1016/B978-0-08-098353-0.00003-8.
- (67) Kuhl, K. P.; Cave, E. R.; Abram, D. N.; Jaramillo, T. F. New Insights into the Electrochemical Reduction of Carbon Dioxide on Metallic Copper Surfaces. *Energy Environ. Sci.* **2012**, *5* (5), 7050–7059.
- (68) Ross, M. B.; De Luna, P.; Li, Y.; Dinh, C. T.; Kim, D.; Yang, P.; Sargent, E. H. Designing Materials for Electrochemical Carbon Dioxide Recycling. *Nat. Catal.* **2019**, *2* (8), 648–658.
- (69) Xiao, J. D.; Jiang, H. L. Metal-Organic Frameworks for Photocatalysis and Photothermal Catalysis. *Acc. Chem. Res.* **2019**, *52* (2), 356–366.
- (70) Nguyen, H. L. Reticular Materials for Artificial Photoreduction of CO₂. *Adv. Energy Mater.* **2020**, *2002091*, 1–23.
- (71) Al-Rowaili, F. N.; Jamal, A.; Ba Shammakh, M. S.; Rana, A. A Review on Recent Advances for Electrochemical Reduction of Carbon Dioxide to Methanol Using Metal-Organic Framework (MOF) and

Non-MOF Catalysts: Challenges and Future Prospects. *ACS Sustain. Chem. Eng.* **2018**, *6* (12), 15895–15914.

(72) Wang, R.; Kapteijn, F.; Gascon, J. Engineering Metal-Organic Frameworks for the Electrochemical Reduction of CO₂: A Minireview. *Chem. - An Asian J.* **2019**, *14* (20), 3452–3461.

(73) Li, D.; Kassymova, M.; Cai, X.; Zang, S. Q.; Jiang, H. L. Photocatalytic CO₂ Reduction over Metal-Organic Framework-Based Materials. *Coord. Chem. Rev.* **2020**, *412*, 213262.

(74) Chen, Y.; Wang, D.; Deng, X.; Li, Z. Metal-Organic Frameworks (MOFs) for Photocatalytic CO₂ Reduction. *Catal. Sci. Technol.* **2017**, *7* (21), 4893–4904.

(75) Nitopi, S.; Bertheussen, E.; Scott, S. B.; Liu, X.; Engstfeld, A. K.; Horch, S.; Seger, B.; Stephens, I. E. L.; Chan, K.; Hahn, C.; Nørskov, J. K.; Jaramillo, T. F.; Chorkendorff, I. Progress and Perspectives of Electrochemical CO₂ Reduction on Copper in Aqueous Electrolyte. *Chem. Rev.* **2019**, *119* (12), 7610–7672.

(76) Alberio, J.; Peng, Y.; García, H. Photocatalytic CO₂ Reduction to C₂⁺ Products. *ACS Catal.* **2020**, *10* (10), 5734–5749.

(77) Gao, D.; Arán-Ais, R. M.; Jeon, H. S.; Roldan Cuenya, B. Rational Catalyst and Electrolyte Design for CO₂ Electroreduction towards Multicarbon Products. *Nat. Catal.* **2019**, *2* (3), 198–210.

(78) Fei, H.; Sampson, M. D.; Lee, Y.; Kubiak, C. P.; Cohen, S. M. Photocatalytic CO₂ Reduction to Formate Using a Mn(I) Molecular Catalyst in a Robust Metal-Organic Framework. *Inorg. Chem.* **2015**, *54* (14), 6821–6828.

(79) Zheng, Y.; Vasileff, A.; Zhou, X.; Jiao, Y.; Jaroniec, M.; Qiao, S. Z. Understanding the Roadmap for Electrochemical Reduction of CO₂ to Multi-Carbon Oxygenates and Hydrocarbons on Copper-Based Catalysts. *J. Am. Chem. Soc.* **2019**, *141* (19), 7646–7659.

(80) Martínez, S.; Veth, L.; Lainer, B.; Dydio, P. Challenges and Opportunities in Multicatalysis. *ACS Catal.* **2021**, *11* (7), 3891–3915.

(81) Ting, L. R. L.; Piqué, O.; Lim, S. Y.; Tanhaei, M.; Calle-Vallejo, F.; Ye, B. S. Enhancing CO₂ Electroreduction to Ethanol on Copper-Silver Composites by Opening an Alternative Catalytic Pathway. *ACS Catal.* **2020**, *10* (7), 4059–4069.

(82) Fan, L.; Xia, C.; Yang, F.; Wang, J.; Wang, H.; Lu, Y. Strategies in Catalysts and Electrolyzer Design for Electrochemical CO₂ Reduction toward C₂⁺ Products. *Sci. Adv.* **2020**, *6* (8), 1–18.

(83) Abdel-Mageed, A. M.; Rungtaweeworant, B.; Parlinska-Wojtan, M.; Pei, X.; Yaghi, O. M.; Behm, R. J. Highly Active and Stable Single-Atom Cu Catalysts Supported by a Metal-Organic Framework. *J. Am. Chem. Soc.* **2019**, *141* (13), 5201–5210.

(84) Zhang, T.; Chen, Z.; Walsh, A. G.; Li, Y.; Zhang, P. Single-Atom Catalysts Supported by Crystalline Porous Materials: Views from the Inside. *Adv. Mater.* **2020**, *32* (44), 1–29.

(85) Yang, Y.; Zhang, X.; Kanchanakungwankul, S.; Lu, Z.; Noh, H.; Syed, Z. H.; Farha, O. K.; Truhlar, D. G.; Hupp, J. T. Unexpected “Spontaneous” Evolution of Catalytic, MOF-Supported Single Cu(II) Cations to Catalytic, MOF-Supported Cu(0) Nanoparticles. *J. Am. Chem. Soc.* **2020**, *142* (50), 21169–21177.

(86) Zhu, Y.; Zheng, J.; Ye, J.; Cui, Y.; Koh, K.; Kovarik, L.; Camaioni, D. M.; Fulton, J. L.; Truhlar, D. G.; Neurock, M.; Cramer, C. J.; Gutiérrez, O. Y.; Lercher, J. A. Copper-Zirconia Interfaces in UiO-66 Enable Selective Catalytic Hydrogenation of CO₂ to Methanol. *Nat. Commun.* **2020**, *11*, 5849.

(87) Masoomi, M. Y.; Morsali, A.; Dhakshinamoorthy, A.; Garcia, H. Mixed-Metal MOFs: Unique Opportunities in Metal-Organic Framework (MOF) Functionality and Design. *Angew. Chemie - Int. Ed.* **2019**, *58* (43), 15188–15205.

(88) Abednatanzi, S.; Gohari Derakhshandeh, P.; Depauw, H.; Coudert, F. X.; Vrielinck, H.; Van Der Voort, P.; Leus, K. Mixed-Metal Metal-Organic Frameworks. *Chem. Soc. Rev.* **2019**, *48* (9), 2535–2565.

(89) Ji, P.; Feng, X.; Oliveres, P.; Li, Z.; Murakami, A.; Wang, C.; Lin, W. Strongly Lewis Acidic Metal-Organic Frameworks for Continuous Flow Catalysis. *J. Am. Chem. Soc.* **2019**, *141* (37), 14878–14888.

(90) Ma, X.; Liu, H.; Yang, W.; Mao, G.; Zheng, L.; Jiang, H. L. Modulating Coordination Environment of Single-Atom Catalysts and

Their Proximity to Photosensitive Units for Boosting MOF Photocatalysis. *J. Am. Chem. Soc.* **2021**, *143* (31), 12220–12229.

(91) Pan, H.; Barile, C. J. Electrochemical CO₂ Reduction to Methane with Remarkably High Faradaic Efficiency in the Presence of a Proton Permeable Membrane. *Energy Environ. Sci.* **2020**, *13* (10), 3567–3578.

(92) Junge Puring, K.; Evers, O.; Prokein, M.; Siegmund, D.; Scholten, F.; Mölders, N.; Renner, M.; Roldan Cuenya, B.; Petermann, M.; Weidner, E.; Apfel, U. P. Assessing the Influence of Supercritical Carbon Dioxide on the Electrochemical Reduction of Formic Acid Using Carbon-Supported Copper Catalysts. *ACS Catal.* **2020**, *10* (21), 12783–12789.

(93) Deria, P.; Gómez-Gualdrón, D. A.; Hod, I.; Snurr, R. Q.; Hupp, J. T.; Farha, O. K. Framework-Topology-Dependent Catalytic Activity of Zirconium-Based (Porphinato)Zinc(II) MOFs. *J. Am. Chem. Soc.* **2016**, *138* (43), 14449–14457.

(94) Chu, W. Y.; Culakova, Z.; Wang, B. T.; Goldberg, K. I. Acid-Assisted Hydrogenation of CO₂ to Methanol in a Homogeneous Catalytic Cascade System. *ACS Catal.* **2019**, *9* (10), 9317–9326.

(95) Huff, C. A.; Sanford, M. S. Cascade Catalysis for the Homogeneous Hydrogenation of CO₂ to Methanol. *J. Am. Chem. Soc.* **2011**, *133* (45), 18122–18125.

(96) Rayder, T. M.; Bensalah, A. T.; Li, B.; Byers, J. A.; Tsung, C. K. Engineering Second Sphere Interactions in a Host-Guest Multicomponent Catalyst System for the Hydrogenation of Carbon Dioxide to Methanol. *J. Am. Chem. Soc.* **2021**, *143* (3), 1630–1640.

(97) Rayder, T. M.; Adillon, E. H.; Byers, J. A.; Tsung, C. K. A Bioinspired Multicomponent Catalytic System for Converting Carbon Dioxide into Methanol Autocatalytically. *Chem.* **2020**, *6* (7), 1742–1754.

(98) Zhang, T.; Manna, K.; Lin, W. Metal-Organic Frameworks Stabilize Solution-Inaccessible Cobalt Catalysts for Highly Efficient Broad-Scope Organic Transformations. *J. Am. Chem. Soc.* **2016**, *138* (9), 3241–3249.

(99) Lan, G.; Li, Z.; Veroneau, S. S.; Zhu, Y. Y.; Xu, Z.; Wang, C.; Lin, W. Photosensitizing Metal-Organic Layers for Efficient Sunlight-Driven Carbon Dioxide Reduction. *J. Am. Chem. Soc.* **2018**, *140* (39), 12369–12373.

(100) Ryu, U. J.; Kim, S. J.; Lim, H. K.; Kim, H.; Choi, K. M.; Kang, J. K. Synergistic Interaction of Re Complex and Amine Functionalized Multiple Ligands in Metal-Organic Frameworks for Conversion of Carbon Dioxide. *Sci. Rep.* **2017**, *7* (1), 1–8.

(101) Su, Y.; Zhang, Z.; Liu, H.; Wang, Y. Cd_{0.2}Zn_{0.8}S@UiO-66-NH₂ Nanocomposites as Efficient and Stable Visible-Light-Driven Photocatalyst for H₂ Evolution and CO₂ Reduction. *Appl. Catal. B Environ.* **2017**, *200*, 448–457.

(102) Zhang, Z. M.; Zhang, T.; Wang, C.; Lin, Z.; Long, L. S.; Lin, W. Photosensitizing Metal-Organic Framework Enabling Visible-Light-Driven Proton Reduction by a Wells-Dawson-Type Polyoxometalate. *J. Am. Chem. Soc.* **2015**, *137* (9), 3197–3200.

(103) Hou, C.-C.; Li, T.-T.; Cao, S.; Chen, Y.; Fu, W.-F. Incorporation of a [Ru(Dcbpy)(Bpy)₂]²⁺ Photosensitizer and a Pt(Dcbpy)Cl₂ Catalyst into Metal-Organic Frameworks for Photocatalytic Hydrogen Evolution from Aqueous Solution. *J. Mater. Chem. A* **2015**, *3* (19), 10386–10394.

(104) Pullen, S.; Fei, H.; Orthaber, A.; Cohen, S. M.; Ott, S. Enhanced Photochemical Hydrogen Production by a Molecular Diiron Catalyst Incorporated into a Metal-Organic Framework. *J. Am. Chem. Soc.* **2013**, *135* (45), 16997–17003.

(105) Dong, Y. J.; Liao, J. F.; Kong, Z. C.; Xu, Y. F.; Chen, Z. J.; Chen, H. Y.; Kuang, D. -B.; Fenske, D.; Su, C. Y. Conformal Coating of Ultrathin Metal-Organic Framework on Semiconductor Electrode for Boosted Photoelectrochemical Water Oxidation. *Appl. Catal. B Environ.* **2018**, *237* (March), 9–17.

(106) Wang, C.; Dekrafft, K. E.; Lin, W.; Kathryn, E.; Lin, W.; Dekrafft, K. E.; Lin, W. Pt Nanoparticles@photoactive Metal-Organic Frameworks: Efficient Hydrogen Evolution via Synergistic Photoexcitation and Electron Injection. *J. Am. Chem. Soc.* **2012**, *134* (17), 7211–7214.

- (107) Yang, S.; Fan, D.; Hu, W.; Pattengale, B.; Liu, C.; Zhang, X.; Huang, J. Elucidating Charge Separation Dynamics in a Hybrid Metal-Organic Framework Photocatalyst for Light-Driven H₂ Evolution. *J. Phys. Chem. C* **2018**, *122* (6), 3305–3311.
- (108) Kim, D.; Whang, D. R.; Park, S. Y. Self-Healing of Molecular Catalyst and Photosensitizer on Metal-Organic Framework: Robust Molecular System for Photocatalytic H₂ Evolution from Water. *J. Am. Chem. Soc.* **2016**, *138* (28), 8698–8701.
- (109) Horiuchi, Y.; Toyao, T.; Miyahara, K.; Zakary, L.; Van, D. Do; Kamata, Y.; Kim, T. H.; Lee, S. W.; Matsuoka, M. Visible-Light-Driven Photocatalytic Water Oxidation Catalysed by Iron-Based Metal-Organic Frameworks. *Chem. Commun.* **2016**, 52 (29), 5190–5193.
- (110) Guo, W.; Lv, H.; Chen, Z.; Sullivan, K. P.; Lauinger, S. M.; Chi, Y.; Sumliner, J. M.; Lian, T.; Hill, C. L. Self-Assembly of Polyoxometalates, Pt Nanoparticles and Metal-Organic Frameworks into a Hybrid Material for Synergistic Hydrogen Evolution. *J. Mater. Chem. A* **2016**, *4* (16), 5952–5957.
- (111) Howarth, A. J.; Liu, Y.; Li, P.; Li, Z.; Wang, T. C.; Hupp, J. T.; Farha, O. K. Chemical, Thermal and Mechanical Stabilities of Metal-Organic Frameworks. *Nat. Rev. Mater.* **2016**, *1* (15018), 1–15.
- (112) Yuan, S.; Feng, L.; Wang, K.; Pang, J.; Bosch, M.; Lollar, C.; Sun, Y.; Qin, J.; Yang, X.; Zhang, P.; Wang, Q.; Zou, L.; Zhang, Y.; Zhang, L.; Fang, Y.; Li, J.; Zhou, H. C. Stable Metal-Organic Frameworks: Design, Synthesis, and Applications. *Adv. Mater.* **2018**, *30* (37), 1704303.
- (113) Schneider, J.; Bahnemann, D. W. Undesired Role of Sacrificial Reagents in Photocatalysis. *J. Phys. Chem. Lett.* **2013**, *4* (20), 3479–3483.
- (114) Sörensen, M.; Zurell, S.; Frimmel, F. H. Degradation Pathway of the Photochemical Oxidation of Ethylenediaminetetraacetate (EDTA) in the UV/H₂O₂-Process. *Acta Hydrochim. Hydrobiol.* **1998**, *26* (2), 109–115.
- (115) Babey, P. A.; Emilio, C. A.; Ferreyra, R. E.; Gautier, E. A.; Gettar, R. T.; Litter, M. I. Kinetics and Mechanisms of EDTA Photocatalytic Degradation with TiO₂. *Water Sci. Technol.* **2001**, *44* (5), 179–185.
- (116) Bhattacharya, M.; Chandler, K. J.; Geary, J.; Saouma, C. T. The Role of Leached Zr in the Photocatalytic Reduction of CO₂ to Formate by Derivatives of UiO-66 Metal Organic Frameworks. *Dalt. Trans.* **2020**, 49 (15), 4751–4757.
- (117) Sampaio, R. N.; Grills, D. C.; Polyansky, D. E.; Szalda, D. J.; Fujita, E. Unexpected Roles of Triethanolamine in the Photochemical Reduction of CO₂ to Formate by Ruthenium Complexes. *J. Am. Chem. Soc.* **2020**, *142* (5), 2413–2428.
- (118) Pellegrin, Y.; Odobel, F. Sacrificial Electron Donor Reagents for Solar Fuel Production. *Chem. Reports* **2017**, *20* (3), 283–295.
- (119) Benseghir, Y.; Solé-Daura, A.; Cairnie, D. R.; Duguet, M.; Mialane, P.; Gairola, P.; Gomez-Mingot, M.; Fontecave, M.; Iovan, D.; Bonnett, B.; Morris, A. J.; Dolbecq, A.; Mellot-Draznieks, C. Unveiling the mechanism of the photocatalytic reduction of CO₂ to formate promoted by porphyrinic Zr-based metal-organic frameworks. *J. Mater. Chem. A* **2022**, Advance Article. DOI: 10.1039/D2TA04164B.
- (120) Wang, Q.; Zhang, Y.; Lin, H.; Zhu, J. Recent Advances in Metal-Organic Frameworks for Photo-/Electrocatalytic CO₂ Reduction. *Chem. - A Eur. J.* **2019**, *25* (62), 14026–14035.
- (121) Dutta, R.; Shrivastav, R.; Srivastava, M.; Verma, A.; Saxena, S.; Biswas, N. K.; Satsangi, V. R.; Dass, S. MOFs in Photoelectrochemical Water Splitting: New Horizons and Challenges. *Int. J. Hydrogen Energy* **2022**, *47* (8), 5192–5210.
- (122) Deng, X.; Li, R.; Wu, S.; Wang, L.; Hu, J.; Ma, J.; Jiang, W.; Zhang, N.; Zheng, X.; Gao, C.; Wang, L.; Zhang, Q.; Zhu, J.; Xiong, Y. Metal-Organic Framework Coating Enhances the Performance of Cu₂O in Photoelectrochemical CO₂ Reduction. *J. Am. Chem. Soc.* **2019**, *141* (27), 10924–10929.
- (123) Zhang, W.; Li, R.; Zhao, X.; Chen, Z.; Law, A. W. K.; Zhou, K. A Cobalt-Based Metal-Organic Framework as Cocatalyst on BiVO₄ Photoanode for Enhanced Photoelectrochemical Water Oxidation. *ChemSusChem* **2018**, *11* (16), 2710–2716.
- (124) Kaye, S. S.; Dailly, A.; Yaghi, O. M.; Long, J. R. Impact of Preparation and Handling on the Hydrogen Storage Properties of Zn₄O(1,4-Benzenedicarboxylate)₃ (MOF-5). *J. Am. Chem. Soc.* **2007**, *129* (46), 14176–14177.
- (125) Panella, B.; Hirscher, M. Hydrogen Physisorption in Metal-Organic Porous Crystals. *Adv. Mater.* **2005**, *17* (5), 538–541.
- (126) Bosch, M.; Zhang, M.; Zhou, H.-C. Increasing the Stability of Metal-Organic Frameworks. *Adv. Chem.* **2014**, 2014, 1–8.
- (127) Chu, J.; Ke, F. S.; Wang, Y.; Feng, X.; Chen, W.; Ai, X.; Yang, H.; Cao, Y. Facile and Reversible Digestion and Regeneration of Zirconium-Based Metal-Organic Frameworks. *Commun. Chem.* **2020**, *3* (1), 1–7.
- (128) Safy, M. E. A.; Amin, M.; Haikal, R. R.; Elshazly, B.; Wang, J.; Wang, Y.; Wöll, C.; Alkordi, M. H. Probing the Water Stability Limits and Degradation Pathways of Metal-Organic Frameworks. *Chem. - A Eur. J.* **2020**, *26* (31), 7109–7117.
- (129) DeCoste, J. B.; Peterson, G. W.; Jasuja, H.; Glover, T. G.; Huang, Y. G.; Walton, K. S. Stability and Degradation Mechanisms of Metal-Organic Frameworks Containing the Zr₆O₄(OH)₄ Secondary Building Unit. *J. Mater. Chem. A* **2013**, *1* (18), S642.
- (130) Doménech, A.; García, H.; Doménech-Carbó, M. T.; Llabrés-i-Xamena, F. Electrochemistry of Metal-Organic Frameworks: A Description from the Voltammetry of Microparticles Approach. *J. Phys. Chem. C* **2007**, *111* (37), 13701–13711.
- (131) Dreischarf, A. C.; Lammert, M.; Stock, N.; Reinsch, H. Green Synthesis of Zr-CAU-28: Structure and Properties of the First Zr-MOF Based on 2,5-Furandicarboxylic Acid. *Inorg. Chem.* **2017**, *56* (4), 2270–2277.
- (132) Zhu, J.; Usov, P. M.; Xu, W.; Celis-Salazar, P. J.; Lin, S.; Kessinger, M. C.; Landaverde-Alvarado, C.; Cai, M.; May, A. M.; Slebodnick, C.; Zhu, D.; Senanayake, S. D.; Morris, A. J. A New Class of Metal-Cyclam-Based Zirconium Metal-Organic Frameworks for CO₂ Adsorption and Chemical Fixation. *J. Am. Chem. Soc.* **2018**, *140* (3), 993–1003.
- (133) Gómez-Gualdrón, D. A.; Moghadam, P. Z.; Hupp, J. T.; Farha, O. K.; Snurr, R. Q. Application of Consistency Criteria to Calculate BET Areas of Micro- and Mesoporous Metal-Organic Frameworks. *J. Am. Chem. Soc.* **2016**, *138* (1), 215–224.
- (134) Momma, K.; Izumi, F. IUCr. VESTA 3 for Three-Dimensional Visualization of Crystal, Volumetric and Morphology Data. *J. Appl. Crystallogr.* **2011**, *44* (6), 1272–1276.